The Journal of Engineering

The 14th IET International Conference on AC and DC Power Transmission (ACDC 2018)

IET Journals
The Institution of Engineering and Technology

DAB-based PET in MVDC traction and shipboard applications with distribution and redundant control

eISSN 2051-3305
Received on 22nd August 2018
Accepted on 19th September 2018
E-First on 4th January 2019
doi: 10.1049/joe.2018.8439
www.ietdl.org

Wang You[1] ✉, *Zheng Zedong*[1], *Li Yongdong*[1]

[1]*Department of Electrical Engineering, Tsinghua University, Beijing, People's Republic of China*

✉ *E-mail: youw94@163.com*

Abstract: Medium-voltage DC (MVDC) grid has drawn more interest in the application of traction and large-scale ships, for its lower loss, higher reliability, higher controllability and simpler system architecture. DC breaker and DC distribution are the key elements in the MVDC grid, and the power electronic transformers (PETs) have shown great advantage in the MVDC grid for its relatively smaller volume and higher flexibility compared to the traditional line transformers and AC/DC converters. In this study, a distribution DC PET based on input series output parallel dual active bridge (DAB) is proposed in the application of power supply system in traction and large scale ships. The DC PET consists of 12 DABs with an input voltage of 10 kV and the output voltage of 380 V. Strategies are proposed for distributed voltage balancing and redundancy control in the proposed PET. Simulations were done in MATLAB/Simulink. In the simulation, waveforms in the normal working conditions and the module fault status is shown, and the result shows that the proposed DC PET has great controllability and flexibility and by adding redundant modules, it keeps great reliability while fault occurs.

1 Introduction

In order to achieve higher power density and efficiency, better operational performance and easier overall design, the integrated power system (IPS) has been paying more attention in the recent years for its advantages in shipboard applications. Although medium-voltage AC (MVAC) systems have been widely studied as the solution for IPS in ships [1], the stability of the system may be affected for the working conditions of the prime mover will change according to the speed and load conditions and the power quality problems highlights with the increasing use of power electronic equipment.

Fig. 1 shows the simplified system structure of the IPS employing medium-voltage DC (MVDC) system. In the IPS, all the equipment are connected to the MVDC bus with AD/DC or DC/DC converters. Compared to the MVAC systems, MVDC systems have the following advantages:

- The AC generator connects the MVDC bus with the AC/DC converter, which enables the use of multiphase motor, enlarging the power capacity and the reliability of the system.
- As all the AC generators are connected through the DC bus, there will be no synchronisation problems.
- The employment of a DC system decouples the operating speed of generators from loads, improving the stability of the system.

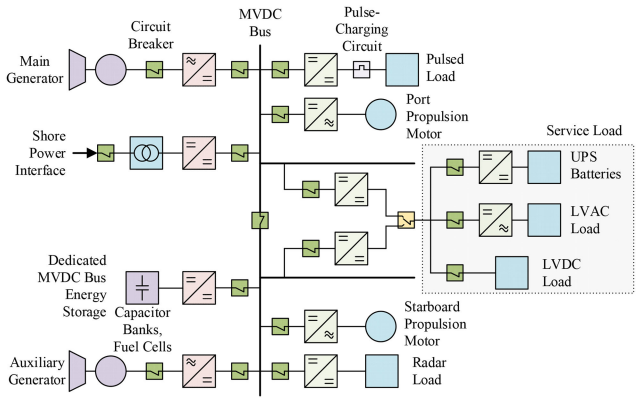

Fig. 1 *Simplified system structure of the IPS employing MVDC system*

- Energy storage like UPS batteries are fuel cells that are simple to connect to the system through the DC buses.
- MVDC system provides cable saving and can deliver power with higher efficiency due to smaller line loss.
- MVDC system provides reactive power suppression, offering a better power quality.

Compared to MVAC system, MVDC systems are of higher efficiency, power quality and reliability [2], and MVDC systems or hybrid MVDC systems are considered as the next generation system architecture in shipboard applications, and have been adopted in industry and navy [3–5]. In MVDC systems, DC breaker and DC distribution are the key part, and it is essential for DC transformers to be of less weight, smaller volume, higher efficiency and reliability.

The structure of the high-speed rail power supply is shown in Fig. 2. The train is powered by a single-phase MVAC grid. Traction transformers are required to convert the single phase MVAC power to one or more isolated low-voltage DC (LVDC) power and requires high quality in input AC current and low harmonics in output DC voltage. As the traction transformers are usually installed in electric locomotives or under the floor of electric multiple units, they not only have strict requirements for volume and weight but also require high reliability and simple control, as well as a certain capacity of redundancy and fault tolerance [6, 7].

Power electronics transformers (PETs) consist of power electronics converters and high-frequency transformer, and are with flexible topology [8]. Compared to conventional transformers with line frequency transformers, PET has the advantages of less weight and smaller volume due to the use of high frequency transformers, and has the ability of reactive power and harmonics compensation, energy management and fault protection due to the use of power electronic converters, which is the ideal solution for DC transformers in shipboard MVDC system and traction transformers in high-speed rail power supply. Both shipboard MVDC system and traction PET require voltage transmission from MVDC/MVAC to LVDC, so DC PETs with large voltage conversion ratio is of important research significance, especially when the traction PET is of AC–DC–DC structure, which has been widely adopted in industrial applications [6].

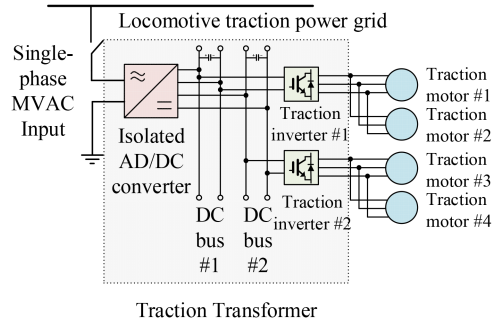

Fig. 2 *Structure of the high-speed rail power supply*

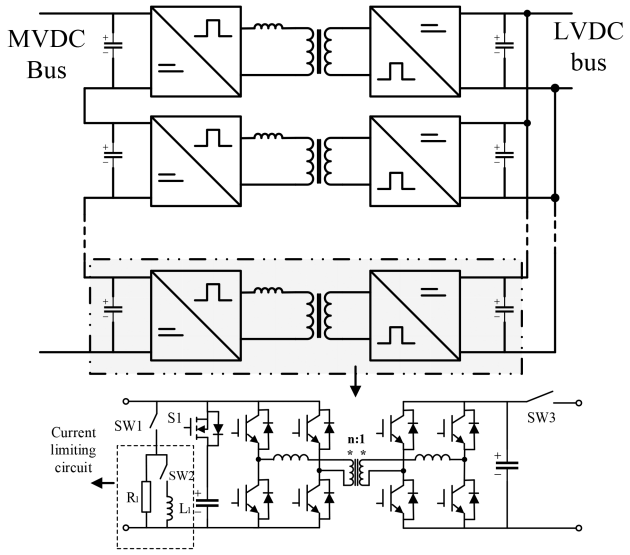

Fig. 3 *Proposed topology of MVDC PET*

So in this paper, a distribution DC PET based on input series output parallel (ISOP) dual active bridge (DAB) is proposed in the application of a power supply system in traction and large scale ships. The working principles of DAB are demonstrated, and the distributed balancing control as well as redundancy control strategies of the ISOP systems are provided in order to ensure the reliability of the system in normal and fault conditions. Simulations are done in MATLAB/Simulink and PLECS with a DC PET consisting of 12 ISOP DABs. The simulation results show that with the given control strategy, the proposed PET can achieve bidirectional power flow in the MVDC system, balanced power flow in each DAB, and stable operation in the fault conditions.

2 Topologies and working principles

2.1 Selection of topologies

From Section 1, there are several considerations for choosing the DC PET topology in shipboard or traction medium-voltage (MV) system, which are listed as follows:

- MV level of at least 10 kV should be achieved on the MV side, and the topology should be easily extended to the higher voltage level.
- As the PET converts MVDC to LVDC, high-voltage gain should be achieved.
- Bidirectional power flow should be achieved, for the energy feedback is required in the MVDC system to achieve higher system efficiency.

Owing to the limited voltage level of the Si-based insulated gate bipolar transistor (IGBT), the topology of the MV side has to be cascaded or multilevel. ISOP topology is considered to be the ideal solution for achieving both high voltage level on the MVDC side and high voltage conversion ratio, and as the sub-modules are of the same topology, it is easy for modular design and expansion. So,

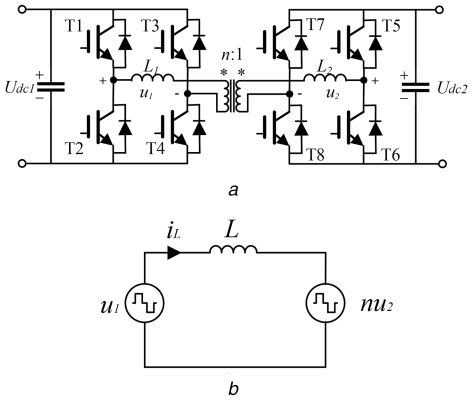

Fig. 4 *Circuit topology and equivalent model of DAB*
(a) Topology of DAB, ***(b)*** Equivalent circuit of DAB

the ISOP topology is chosen as the system topology, and the control strategy will be discussed in Section 3.

As to the sub-module, DAB can achieve smooth bidirectional power by adjusting the phase shift angle between the primary side and secondary side output. Compared to other isolated DC/DC converters, DAB has a strong regulatory capacity for the transmission power and output voltage and can achieve flexible control. So the DAB is chosen as the sub-module topology, and the working principles will be discussed in Section 2.2.

As mentioned above, the proposed topology of the DC PET is shown in Fig. 3. The PET consists of ISOP DABs, with a protection switch on the input side and on the output side of each DAB.

2.2 Working principles of DAB

DAB consists of two H-bridges and a high-frequency transformer, and the topology and simplified equivalent circuit are shown in Fig. 4. In Fig. 4*b*, all the parameters are equivalent to the primary side of the transformer, the IGBTs are considered as an ideal switch, and L contains the leakage inductance and the inductance of the high-frequency transformer. In order to reduce the transformer excitation current loss, the excitation inductance of the transformer is often designed to be large, which can be ignored in the analysis.

The modulation waveforms are shown in Fig. 5. As shown in Fig. 5, there are three variables in the modulation: the internal phase shift δ_1, δ_2 of the two output square waves of the H-bridges and the external phase shift δ_0 between the square waves. The internal phase shift affects the duty cycle of the corresponding square wave and varies between [0, 0.5] and the external phase shift affects the phase difference between the square waves and varies between [−1, 1]. The modulation strategy of DAB has been studied a lot [9, 10], and in order to reduce the current stress at the switching moment, current stress optimal modulation strategy is adopted in the paper [6], and the relationship between δ_1, δ_2, and δ_0 and the average power flow is shown below:

$$\begin{cases} \overline{p} = \dfrac{nU_{\mathrm{dc1}}U_{\mathrm{dc2}}}{2fL_s}(1-2\delta_2)\delta_0 \\ \delta_1 = 0.5 - \dfrac{d\delta_0}{2(d-1)} \quad , \quad \delta_0 \in \left[0, \dfrac{d-1}{2d}\right], d > 1 \\ \delta_2 = 0.5 - \dfrac{\delta_0}{2(d-1)} \end{cases} \tag{1}$$

$$\begin{cases} \overline{p} = \dfrac{nU_{\mathrm{dc1}}U_{\mathrm{dc2}}}{2fL_s} \\ \qquad \times \left[\delta_0(1-\delta_0) - \delta_1^2 - \delta_2^2\right], \quad \delta_0 \in \left[\dfrac{d-1}{2d}, 0.5\right], \quad d > 1 \\ \delta_1 = 0 \\ \delta_2 = \dfrac{d-1}{2}(1-2\delta_0) \end{cases} \tag{2}$$

$$\begin{cases} \overline{p} = \dfrac{nU_{\mathrm{dc1}}U_{\mathrm{dc2}}}{2fL_s}(1-2\delta_1)\delta_0 \\ \delta_1 = 0.5 - \dfrac{d\delta_0}{2(1-d)} \quad , \quad \delta_0 \in \left[0, \dfrac{1-d}{2}\right], d \le 1 \\ \delta_2 = 0.5 - \dfrac{\delta_0}{2(1-d)} \end{cases} \tag{3}$$

$$\begin{cases} \overline{p} = \dfrac{nU_{\mathrm{dc1}}U_{\mathrm{dc2}}}{2fL_s} \\ \qquad \times \left[\delta_0(1-\delta_0) - \delta_1^2 - \delta_2^2\right], \quad \delta_0 \in \left[\dfrac{1-d}{2}, 0.5\right], d \le 1 \\ \delta_1 = \dfrac{1-d}{2d}(1-2\delta_0) \\ \delta_2 = 0 \end{cases} \tag{4}$$

where d is the voltage gain of DAB.

$$d = \frac{nu_2}{u_1} \tag{5}$$

3 Control strategies

3.1 LV side voltage and ISOP balance control

From Section 2.2, it is known that the power transferred in the DAB can be controlled by adjusting δ_0, and then by expression (1)–(5), δ_1 and δ_2 can be derived. In order to control the LVDC bus voltage, an LV side voltage control loop is adopted. For ISOP systems, power balance of each sub-module is required. Input voltage sharing (IVS) control and output current sharing (OCS) control are often adopted in order to achieve the power balance [11]. Owing to the input of all the sub-modules is series, they have the same input current, if all sub-modules can share the input voltage, they will share the same output current. Also, as the output of all the sub-modules are parallel, they have the same output voltage, if all sub-modules can share the output current, they will share the same input voltage. As analysed above, adopting only one of the IVS or OCS control is enough to achieve the power sharing in the ISOP system. In the paper, IVS control is adopted, and the control strategy of the whole system is shown in Fig. 6.

In Fig. 6, the LV side voltage control loop is the outer control loop. The LV side voltage is compared to the reference value, goes through a PI adapter, and the reference value δ_0 is obtained to keep the LV side voltage to be at the reference value. The balancing control loop is the inner control loop. The reference value of the inner loop is the average input voltage of all the working sub-modules. The input voltage is compared to the reference value and the output of each PI adapter is the correction value of the external phase shift for each sub-module. By adding the reference value δ_0 and the correction value, the final value of the external phase shift for each sub-module is obtained. As there are no coupling terms in each sub-module control loop, distribution control is achieved in the system when keeping the reference LV side voltage and the power balancing.

3.2 ISOP redundant control

When fault occurs in one of the sub-modules, the fault module should be removed from the whole system in order to continue the stable operation. The structure of the fault protection circuit in each sub-module is shown in Fig. 7. In Fig. 7, 3 DC breakers SW1–SW3 are placed in the input and output of the DAB. SW1 is the bypass switch and is disconnected under normal conditions. When the sub-module needs are removed from the system, SW1 is closed. SW3 is to disconnect the sub-module from the LVDC bus. SW3 is closed under normal conditions and disconnected when the sub-module needs to be removed.

When a sub-module is to remove from the ISOP system, SW1 is to close, and there are two reasons causing the overcurrent in SW1. The first is the shortcut of the DC bus capacitor when SW1 is closed, and the second is the voltage mismatch of the input DC

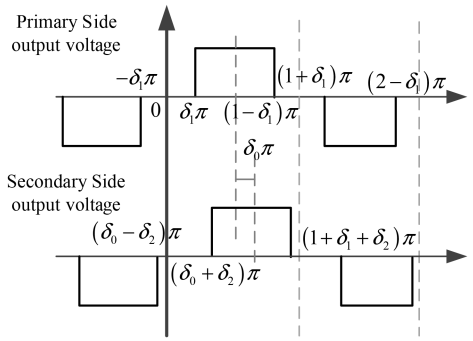

Fig. 5 *Modulation waveforms of DAB*

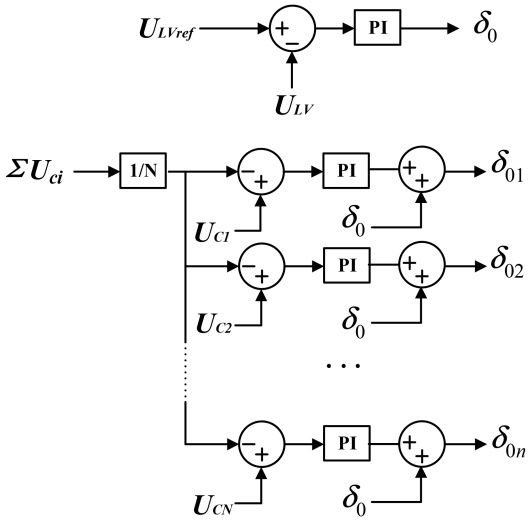

Fig. 6 *Control strategies for ISOP DAB system*

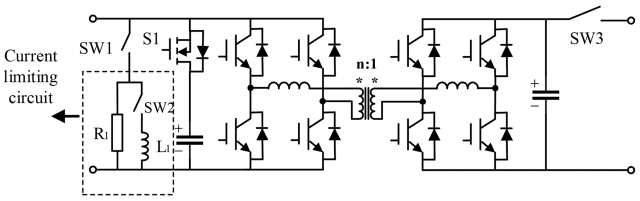

Fig. 7 *Redundant control circuit for DAB sub-modules*

source and the rest series DC bus capacitors. In order to reduce the current spikes when SW1 is closing, a current limiting circuit is proposed in Fig. 7. To limit the overcurrent by the shortcut of the DC bus capacitor a MOSFET with anti-parallel diode S1 is connected series with the capacitor. S1 is closed at normal conditions, and as only ripple current flows through S1, the conduction loss is relatively small. Moreover to limit the overcurrent caused by the voltage mismatch, a limiting resistor R_1 is adopted to charge the rest of the capacitors in the transient stage. As the load current flows through R_1, causing comparatively a large loss, SW2 is closed when the voltage of the DC bus capacitors reach a steady state, and the load current will then flow through the inductance L_1 instead of R_1.

The current limiting control timing is proposed in Fig. 8. In Fig. 8, when a fault occurs in the sub-modules, the gate signal on both sides of DAB is immediately blocked, then the fault signal is received in the main controller, SW1 on signal, S1 off signal is given, and the number of sub-modules and the reference voltage of balancing control loop are refreshed. When SW1 is closed, the rest of the DC bus capacitors are charged with the limiting resistor R_1. When the DC bus voltage reach a steady value, SW2 off signal is given, then SW2 is closed, the load current begin to commutate to the SW2–L_1 branch. As the gate signals of all the switches are blocked right after the fault occurs, there is no current flowing through SW3, and when the transient process of the series side is

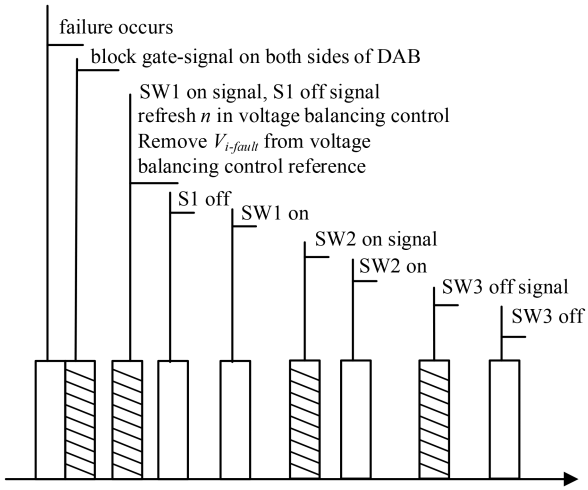

Fig. 8 *Redundant control timing for DAB sub-modules*

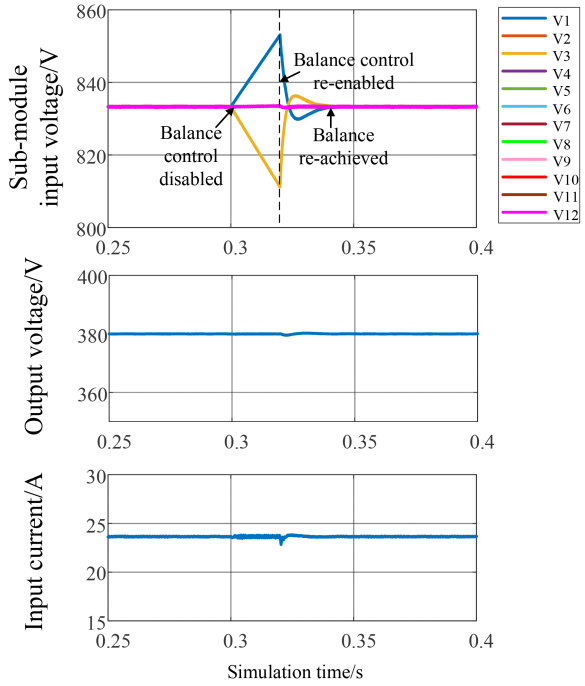

Fig. 9 *Simulation waveforms in steady state*

over, SW3 off signal is sent and then SW3 is disconnected to disconnect the DAB from the LVDC bus.

4 Simulation results

Simulation is done in MATLAB/Simulink and PLECS to verify the effectiveness of the control strategy. In the simulation, the PET consists of 12 ISOP DABs, with the input voltage of 10 kV, the output voltage of 380 V and the total power of 200 kW. Other simulation parameters are listed in Table 1.

The simulation results are shown in Figs. 9 and 10. In Fig. 9, the input voltage of each sub-module and the output voltage of the PET is shown. It can be seen that the output voltage is regulated at 380 V, and the input voltage of each sub-module is well balanced. When $t = 0.3$ s, the balance control was disabled, and the input voltage of each sub-module became immediately unbalanced due to the parameter mismatch of the leakage inductance. The balance control was re-enabled at $t = 0.32$ s, and the input voltage of each sub-module became balanced again within <0.02 s.

In Fig. 10, the input voltage of each sub-module, the output voltage and the input current of the PET is shown. The fault occurred at module 2 when $t = 0.2$ s, and the DAB was stopped when the fault occurs. Due to the on delay of SW1, the voltage of module 2 rise a little before SW1 is on, and the rest of the

Table 1 Simulation parameters of the PET

Parameters	Values
leakage inductance, μH	80 (85 in module 1 and 75 in module 3)
sub-module MVDC bus capacitance, μF	1500
sub-module LVDC bus capacitance, μF	1500
limiting resistance R_1, Ω	10
limiting inductance L_1, mH	10

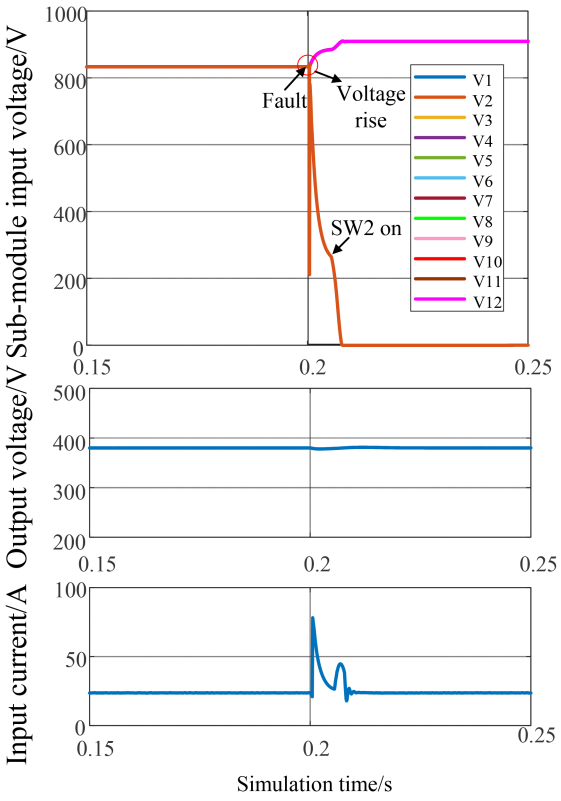

Fig. 10 *Simulation waveforms in fault state*

capacitors was charged by the limiting resistor, and then the load current commutated through the limiting inductor and SW2. It can be seen in Fig. 10 that the overcurrent was limited to an acceptable value and the output voltage fluctuation was very small during the transient state.

5 Conclusion

In the paper, a DAB-based ISOP DC PET is proposed for the application of MVDC system in shipboard and traction. Working principles are discussed and control strategies are proposed for the ISOP balancing and fault conditions. The simulation result shows that all the submodules share the same input voltage despite the parameter mismatch, and the output voltage is regulated to the reference value. By applying the fault state control, the PET can remove the fault module with acceptable current spike and little fluctuation in the output voltage.

6 Acknowledgments

The paper was sponsored by the National Key Research and Development Plan (2017YFB1200901-12), and Beijing Natural Science Foundation (316001).

7 References

[1] Bidram, A., Davoudi, A., Lewis, F.L.: 'Distributed control for AC shipboard power systems'. 2013 IEEE Electric Ship Technologies Symp. (ESTS), Arlington, VA, USA, 2013, pp. 282–286

[2] Javaid, U., Dujić, D., van der Merwe, W.: 'MVDC marine electrical distribution: are we ready?'. IECON 2015-41st Annual Conf. of the IEEE Industrial Electronics Society, Yokohama, Japan, 2015, pp. 000823–000828
[3] McCoy, T.J.: 'Integrated power systems – an outline of requirements and functionalities for ships', *Proc. IEEE*, 2015, **103**, (12), pp. 2276–2284
[4] Das, M.K., Capell, C., Grider, D.E., *et al.*: '10 kV, 120 A SiC half H-bridge power MOSFET modules suitable for high frequency, medium voltage applications'. 2011 IEEE Energy Conversion Congress and Exposition (ECCE), Phoenix, AZ, USA, 2011, pp. 2689–2692
[5] Dong, D., Garces, L., Agamy, M., *et al.*: 'Control and operation of medium-voltage high-power bi-directional resonant DC–DC converters in shipboard dc distribution systems'. 2016 IEEE Energy Conversion Congress and Exposition (ECCE), Milwaukee, WI, USA, 2016, pp. 1–9
[6] Gu, C., Zheng, Z., Xu, L., *et al.*: 'Modeling and control of a multiport power electronic transformer (PET) for electric traction applications', *IEEE Trans. Power Electron.*, 2016, **31**, (2), pp. 915–927
[7] Feng, J., Chu, W.Q., Zhang, Z., *et al.*: 'Power electronic transformer-based railway traction systems: challenges and opportunities', *IEEE J. Emerg. Sel. Top. Power Electron.*, 2017, **5**, (3), pp. 1237–1253
[8] Falcones, S., Mao, X., Ayyanar, R.: 'Topology comparison for solid state transformer implementation'. 2010 IEEE Power and Energy Society General Meeting, Minneapolis, MN, USA, 2010
[9] Zhao, B., Yu, Q., Sun, W.: 'Extended-phase-shift control of isolated bidirectional DC–DC converter for power distribution in microgrid', *IEEE Trans. Power Electron.*, 2012, **27**, (11), pp. 4667–4680
[10] Wen, H., Xiao, W.: 'Bidirectional dual-active-bridge DC–DC converter with triple-phase-shift control'. 2013 Twenty-Eighth Annual IEEE Applied Power Electronics Conf. and Exposition (APEC), Long Beach, CA, USA, 2013, pp. 1972–1978
[11] Fang, T., Shen, L., He, W., *et al.*: 'Distributed control and redundant technique to achieve superior reliability for fully modular input-series-output-parallel inverter system', *IEEE Trans. Power Electron.*, 2017, **32**, (1), pp. 723–735